Polymer 150 (2018) 267–274

Contents lists available at ScienceDirect

Polymer

journal homepage: www.elsevier.com/locate/polymer

Excellent thermal stability P(BeA-co-MMA) microcapsules with high thermal energy storage capacity

Yuchen Mao [a, b], Jin Gong [a, *], Meifang Zhu [b, **], Hiroshi Ito [a, ***]

[a] Department of Polymer Science & Engineering, Graduate School of Organic Materials Science, Yamagata University, 4-3-16 Jonan, Yonezawa, Yamagata 992-8510, Japan

[b] State Key Laboratory for Modification of Chemical Fibers and Polymer Materials, College of Materials Science and Engineering, Donghua University, Shanghai 201620, China

ARTICLE INFO

Article history:
Received 19 April 2018
Received in revised form
6 July 2018
Accepted 14 July 2018
Available online 17 July 2018

Keywords:
Crystalline copolymer
Thermoregulation
Microcapsule

ABSTRACT

Low thermal stability and the shortage of core leakage strongly limit the application of conventional energy storage microcapsules. This study focuses on a novel strategy to develop a new phase change material with excellent thermal durability without core leakage. The new phase change materials is a P(BeA-co-MMA) copolymer microcapsule with crystalline *n*-alkane side chains. Under the protection of polymer main chains as the shell or skeleton structure on a nano-scale, the crystalline side chains as the core will no longer suffer loss and will maintain stablity in use. The chemical composition, inner homogeneous structure, thermoregulation properties, crystalline behaviour and thermal stability are discussed. The P(BeA-co-MMA) microcapsules provide energy storage capacity in the temperature range of 48–62 °C with the highest enthalpy of 105.1 J g^{-1}. The 5% weight loss temperature ($T_{5\%}$) is more than 315 °C, which is high enough to withstand the general polymer processing temperature to open the possibility of developing energy storage modified fibre and polymer materials as functional fillers.

1. Introduction

Latent heat storage systems provide a highly efficient and environmentally friendly means to use residual heat and store renewable energy. Phase change materials, which can absorb or release the enthalpy of phase changes in certain temperature ranges, are considered among the most reliable latent heat storage and thermoregulation materials. Phase change materials have been successfully applied in the fields of solar energy, aerospace and aviation, environmental control, and textiles [1,2]. Among phase change materials, paraffin and *n*-alkane are the most popular owing to their characteristics of high phase change enthalpy, high energy storage density, relativly low volume change ratio, good physical and chemical stability, and no super-cooling or phase segregation behaviour [3,4]. More importantly, there are wide selective working temperature ranges that greatly extend their operating conditions.

Microcapsules are considered micro-scale containers to prevent cores from leaking, isolate them from the surroundings, and maintain chemical and functional stability in service. There are several methods to synthesize microcapsules: spray drying [5], complex coacervation [6], sol-gel [7], in-situ polymerization [8–11], suspension polymerization [12–14] and emulsion polymerization [15–17]. Among these, suspension polymerization has the advantages of being simple, cheap, stable, eco-friendly, and easily controlled, which makes it the most popular chemical method to synthesize microcapsules. Most shell materials of conventional microcapsules are synthetic macromolecules, such as urea-formaldehyde resin (UF) [9], melamine-formaldehyde resin (MF) [11,18], polyurea (SPUA) [19], polyurethane (PU) [20], polystyrene (PS) [16], methacrylate-based copolymers [13–15,21] and styrene-based copolymers [22]. The properties of shell materials greatly impact the application and processing conditions of the final energy storage composite materials. Nevertheless, the low thermal stability and physical strength of polymers in nature strongly restrict application fields of microcapsules [15]. What is more, the evaporation or sublimation of core materials causes lower thermal stability.

* Corresponding author.
** Corresponding author.
*** Corresponding author.
E-mail addresses: jingong@yz.yamagata-u.ac.jp (J. Gong), zmf@dhu.edu.cn (M. Zhu), ihiroshi@yz.yamagata-u.ac.jp (H. Ito).

https://doi.org/10.1016/j.polymer.2018.07.040
0032-3861/

To overcome these shortages of shell fracture, core leakage, core evaporation, or sublimation existing in conventional microcapsules, we design a copolymer microcapsule with strong interaction force between shell and core parts and no separated surface layer between shell and core. The strong interaction force between shell and core allows maximal improvement of microcapsule thermal stability. The copolymer microcapsule is synthesized by suspension polymerization of behenyl acrylate (BeA) and methyl methacrylate (MMA) as shown in Fig. 1. The structure of BeA consists of a long alkane chain with 22 methylene units and a vinyl group. The long alkane chain can provide the energy storage capacity, whereas the vinyl group has reactivity to form a polymer with the aid of a radical initiator. PMMA is famous as an amorphous plastic, because the presence of the pendent methyl ($-CH_3$) and acetoxy ($-COOCH_3$) groups prevents the polymer chains from packing closely in a crystalline fashion. On the other hand, it also prevents the polymer chains from rotating freely around the carbon–carbon bonds. The above effects cause PMMA to be a tough and rigid plastic. Therefore, the purpose of introducing MMA is to increase the strength and adjust the phase change temperature of P(BeA-co-MMA) microcapsules. Owing to the low self-polymerization rate of a long chain monomer BeA [23], another purpose of introducing MMA is to increase the polymerization rate and form stable micelles quickly. In this paper, we report the synthesis, size control, and structure analysis of P(BeA-co-MMA) microcapsules, which have both excellent thermal stability and high thermal energy storage capacity.

2. Experiment

2.1. Materials

Monomer BeA was provided by Shin-Nakamura Chemical Co., Ltd., Japan. Another monomer MMA, the oil-soluble initiator 2, 2′-Azobis (2-methylpropionitrile) (AIBN), and methanol were purchased from Wako Pure Chemical Industries, Ltd., Japan. Polyvinyl alcohol (PVA) provided by Kuraray Co., Ltd., Japan was used as an emulsifier. All the above reagents were used without further purification.

2.2. Preparation of P(BeA-co-MMA) microcapsules

Five different microcapsule samples were prepared with varying molar ratios of BeA to MMA by suspension polymerization. The reaction system consisted of two phases, the water phase and the oil phase. Monomers BeA and MMA and part of initiator AIBN were mixed to make the oil phase. The water phase was made by mixing deionized water and PVA solution. The oil phase was then added into the water phase to carry out the microencapsulation at 60 °C under an emulsification rate of 8000 rpm for 60 min. The emulsion was transferred into a three-neck round-bottom flask equipped with a mechanical stirrer and a condensate tube. The emulsion was then heated to 75 °C to initiate the polymerization reaction. To control the reaction rate in the initial stage, MMA and the rest of the AIBN were added dropwise into the emulsion at a stirring rate of 400 rpm for 60 min. After adding the remainder of the oil phase, the emulsion was heated to 85 °C to increase the polymerization reaction rate and speed up the formation of stable micelles. The polymerization was conducted for 4 h under a stirring rate of 600 rpm. The microcapsules were separated from the emulsion by centrifuging at 5000 rpm for 10 min, washed with methanol twice, and then vacuum-dried at 40 °C for 48 h. Finally, the white powder microcapsules were obtained with the yield greater than 60%. We prepared a series of P(BeA-co-MMA) microcapsules in a similar manner with the molar ratios of MMA to BeA of 1:1, 1:2, 1:3, 1:4 and 1:5, which we named MC1, MC2, MC3, MC4 and MC5, respectively.

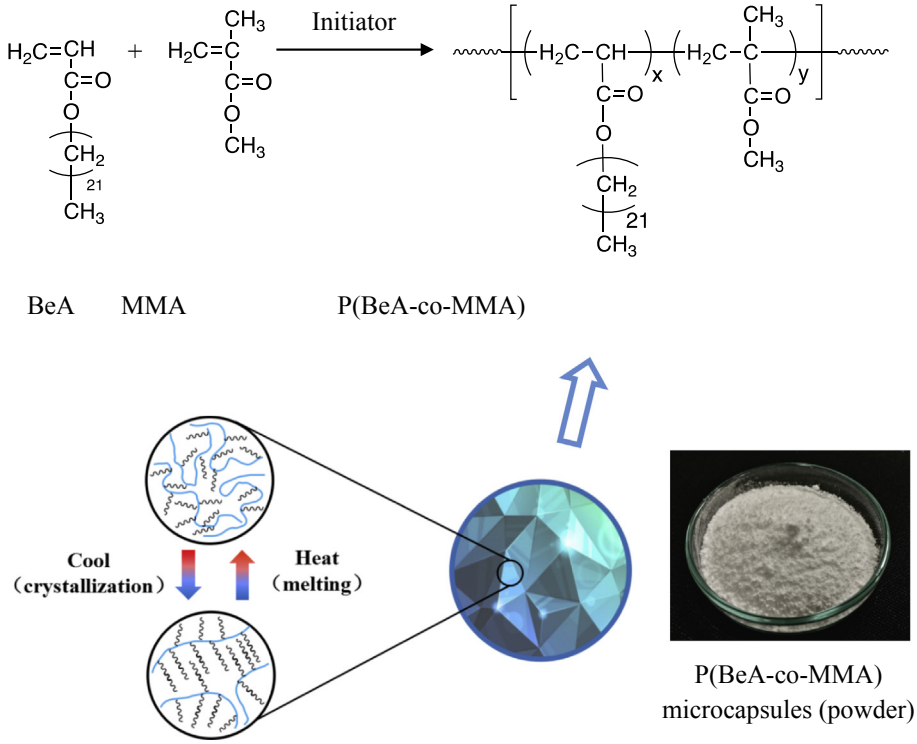

Fig. 1. Scheme of synthesis and phase change mechanism of P(BeA-co-MMA) copolymer microcapsules. The photograph of the synthesized P(BeA-co-MMA) microcapsules is also shown.

2.3. Characterization

The morphology and surface feature of the P(BeA-co-MMA) microcapsules were observed on a scanning electron microscopy (SEM) (JSM-5510, JEOL Ltd, Tokyo, Japan). The specimens were sputter-coated with platinum-palladium for SEM analyses. The particle size distribution (PSD) of microcapsules was measured on a laser diffraction particle size analyzer (SALA-7000, Shimadzu Co., Kyoto, Japan). The laser diffraction spectrometry (LDS) method required that the particles be in a dispersed state. Microcapsule suspension in PVA solution was prepared and used for measurement. The chemical structure was assessed using a Fourier transform infrared spectrometer (FT/IR-460 Plus, JASCO International Co., Ltd., Tokyo, Japan). The wavenumber region was 500 cm^{-1} and 3400 cm^{-1}. The thermal properties and phase change behaviour of the P(BeA-co-MMA) microcapsules were investigated using a Q2000 (TA Instruments Japan Inc., Tokyo, USA) under a nitrogen atmosphere at a heating/cooling rate of 5 °C·min^{-1}. An infrared thermal graphic camera (FLIR E6, FLIR Systems Inc., Wilconville, USA) was used to record the temperature change and evaluate the thermoregulation properties of P(BeA-co-MMA) microcapsules. Heating-cooling cycles of microcapsules were carried out with temperature ranging from 25 to 80 °C on a hot stage (FP82HT hot stage connected to FP90 central processor, Mettler Toledo, USA), and the temperature change rate was set at 5 °C·min^{-1}. The thermal stability and degradation properties were evaluated using thermal gravimetric analysis (TGA) (Q-50, TA instruments Japan Inc., Tokyo, USA). The analysis was conducted under a nitrogen atmosphere at a heating rate of 10 °C·min^{-1} in a temperature range 100–500 °C. Wide angle X-ray scattering (WAXS) was performed on an X-ray diffractometer (Ultima IV, Rigaku Instrument Co., Akishima, Japan) with nickel-filtered Cu Kα radiation at a scanning rate of 5°·min^{-1}.

3. Results and discussion

3.1. Morphology and particle size distribution

The SEM photographs of synthesized P(BeA-co-MMA) microcapsules are shown in Fig. 2. Although the morphology of MC1 is irregular, other microcapsules of MC2–MC5 show uniform spheres. The particle size distribution diagrams of microcapsules measured by the LDS method are also shown in Fig. 2. In addition, we present the diagram of MC3 in Fig. 3 for a clearer understanding as an example for discussion. In the size distribution diagrams, microcapsules exhibit two size distribution peaks, one with a diameter at approximately 100 nm, and one at 1–100 μm. The major diameter range of P(BeA-co-MMA) microcapsules is approximately 10 μm. The small size microcapsules are also spherical, which is considered to be caused by the higher polymerization rate of the monomer MMA than BA [23]. The large size peaks are attributed to microcapsules with large diameter, and their aggregates are due to the aggregation tendency of micro- and nano-sized particles. We also can observe the aggregates of microcapsules in SEM photographs shown in Fig. 2. Next, we analyze the median diameters of microcapsules (d_{50}). The d_{50} value corresponds to 50% of a cumulative distribution and indicates that half the particles are smaller (or larger) than the median. The d_{50} value are 7.15 μm for MC1, 7.34 μm for MC2, 11.61 μm for MC3, 14.75 μm for MC4, and 14.46 μm for MC5. Clearly, the diameter increases with increasing amount of BeA. Further increasing the amount of BeA in turn leads to size reduction for MC5 owing to the unstable emulsion in suspension polymerization.

When observing broken microcapsules (Fig. 2 (f)), the interface between the shell and core was not observed. This indicates that the P(BeA-co-MMA) microcapsules have a homogeneous phase structure. The worrisome leakage problem in conventional shell-core structure microcapsules is avoided and no longer exists in P(BeA-co-MMA) homogeneous microcapsules, because the crystal microcells are maximally protected by the polymer main chain skeleton structure (Fig. 1). Even if the P(BeA-co-MMA) microcapsules broke into pieces, they would maintain their energy storage capacity and not cause any pollution to the surroundings.

3.2. Chemical composition and structure

The chemical composition and structures of P(BeA-co-MMA) microcapsules were evaluated by FTIR spectroscopy, presented in Fig. 4, along with monomer MMA and BeA. P(BeA-co-MMA) microcapsules have a similar spectrum profile containing a series of characteristic absorption derived from monomer MMA and BeA. All microcapsules show strong multiplet intensive absorption peaks at 2957 cm^{-1}, 2920 cm^{-1} and 2850 cm^{-1} owing to the alkyl C-H stretching vibrations of the methyl and methylene group. The C=O stretching vibration of ester triggers a strong intensive absorption peak at 1734 cm^{-1}. The peaks at 1260 cm^{-1}, 1160 cm^{-1} and 1130 cm^{-1} can be assigned to the C-O stretching vibration of the ester group. These characteristic peaks are typical of acrylic ester. There is an absorption band at 1444 cm^{-1}, which is attributed to the C-H bending vibration of the methyl group on the polymer backbone peak derived from MMA, and it becomes weak with a lower amount of MMA. The infrared spectra also exhibits an absorption peak at 722 cm^{-1} corresponding to the in-plane rocking vibration of methylene groups belonging to the long alkane side chain derived from BeA. It is noted that after the polymerization process, the characteristic absorption peak of C=C at 1635 cm^{-1} is absent or becomes weak, which proves the successful synthesis of P(BeA-co-MMA) copolymer microcapsules and that there is a residual of unreacted vinyl group left in the microcapsules.

3.3. Thermal storage capacity

Thermal storage capacity is the key property of phase change materials. The phase change enthalpy (ΔH) is often used to characterize the energy storage capacity. The phase change temperature is also important and impacts the application fields. The phase change behaviour and thermal storage/release capacity of monomer BeA and P(BeA-co-MMA) microcapsules were evaluated by DSC. For comparison, poly(behenyl acrylate) (PBeA) and poly(-methyl methacrylate) (PMMA) were polymerized and also evaluated. The DSC curves in the crystallization and melting processes of BeA, PBeA, PMMA and P(BeA-co-MMA) microcapsules are illustrated in Fig. 5, and more detailed data are summarized in Table 1. Monomer BeA displays a strong and sharp peak and high enthalpy in both crystallization and melting processes owing to its pendent long alkane group. This indicates that BeA has great potential for energy storage applications.

Compared with monomer BeA, both the crystallization temperature (T_c) and melting temperature (T_m) of PBeA increasd by 12.5 °C and 17.5 °C, respectively, while the ΔH reduced 20%. The higher T_c and T_m of PBeA are due to the bond strength and binding force of the carbon–carbon main chain in PBeA. The decrease of ΔH can be ascribed to the decline in crystallization ability of the side chains of PBeA. As reported by Shibasaki et al. [23], in the comb-like polymer, eight or nine methylene units of the side chain in the vicinity of the main chain are amorphous. Thus, it is presumed that only the terminal parts of side chains crystallized in PBeA, leading to the decrease of ΔH.

With increasing amount of BeA, T_m, T_c and ΔH of P(BeA-co-MMA) microcapsules increase. Notably, the ΔH of MC3 reaches

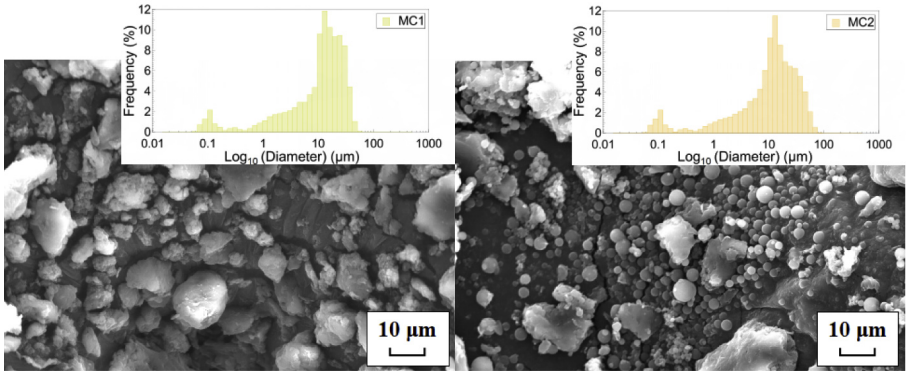

(a) MC1

(b) MC2

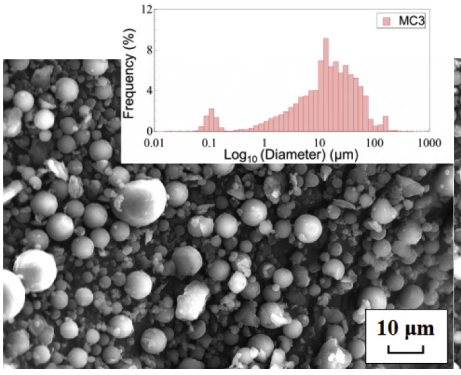

(c) MC3

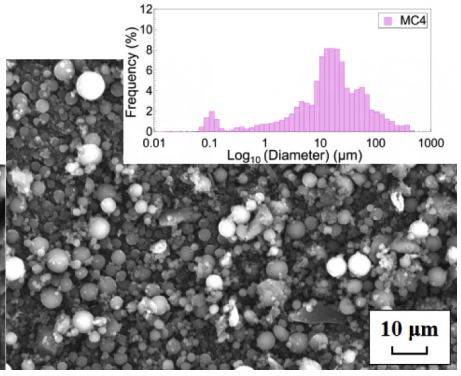

(d) MC4

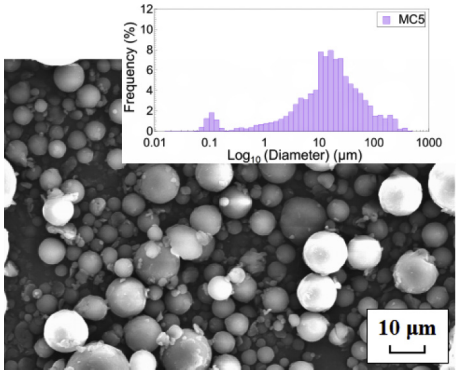

(e) MC5

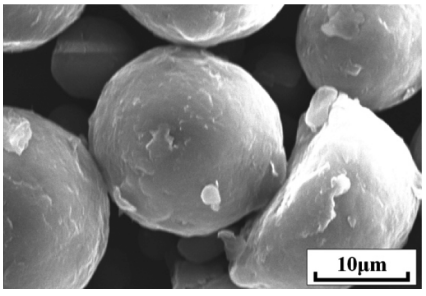

(f) broken microcapsules of MC3

Fig. 2. SEM photographs and particle size distribution diagrams measured by the LDS method for P(BeA-co-MMA) microcapsules. MC1 (a) is irregular, and the other microcapsules of MC2 (b), MC3 (c), MC4 (d), and MC5 (e) are spherical. Broken microcapsule of MC3 (f) show a homogeneous inner structure. The particle size distribution diagrams indicate that the major diameter range of P(BeA-co-MMA) microcapsules is approximately 10 μm.

105.1 J g^{-1}, the highest among all P(BeA-co-MMA) microcapsules. With further increasing of BeA, T_m, T_c and ΔH of MC4 and MC5 do not rise but decrease. The reason is considered to be that under the ratio of MMA:BeA = 1:3, the copolymer chain has enough movement ability to adjust its steric conformation and reduce the steric hindrance, allowing more methylene units to arrange into crystals. Compared to MC3, the chains of MC4 are more rigid, so the side chains cannot easily form a crystal structure at the same cooling rate. For MC5 with the highest BeA amount, its T_m and T_c are close to those of PBeA, whereas ΔH further decreases. The unstable emulsion in suspension polymerization caused by much more BeA is considered to be the cause of the further decrease of ΔH, as with the size decrease of MC5 mentioned above.

To gain a clearer visual understanding of the thermoregulation property, infrared thermal testing was used to evaluate the energy storage capacity. A controlled hot stage with a temperature change rate at 5 °C·min^{-1} was used to carry out the measurement with one heating/cooling cycle. Fig. 6 shows the photographic image and temperature–time curves supplied by an infrared thermal camera. For both heating and cooling processes, the microcapsules show the thermoregulation property to storage phase change energy. A buffer zone in heating/cooling and the temperature differences

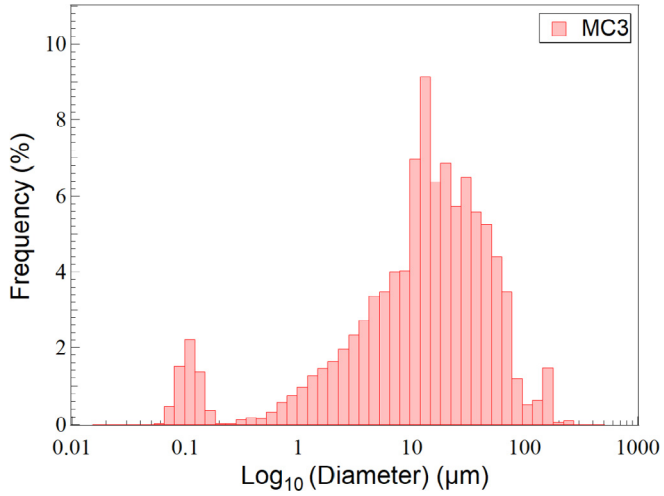

Fig. 3. Particle size distribution measured by the LDS method for microcapsule MC3. It is shown for a clearer understanding as an example.

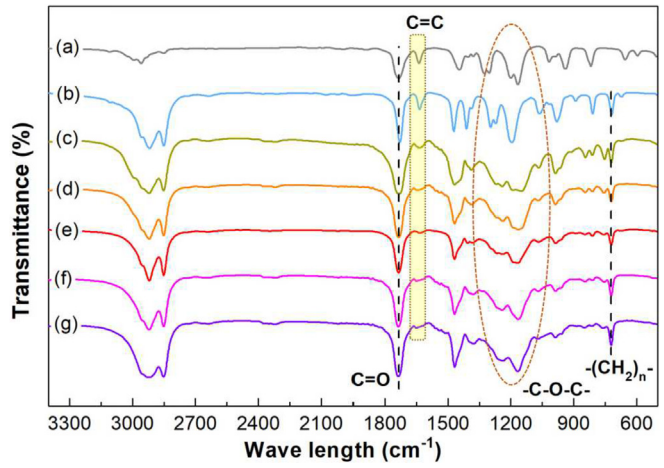

Fig. 4. FTIR spectra of MMA (a), BeA (b), and P(BeA-co-MMA) microcapsules of MC1 (c), MC2 (d), MC3 (e), MC4 (f), and MC5(g).

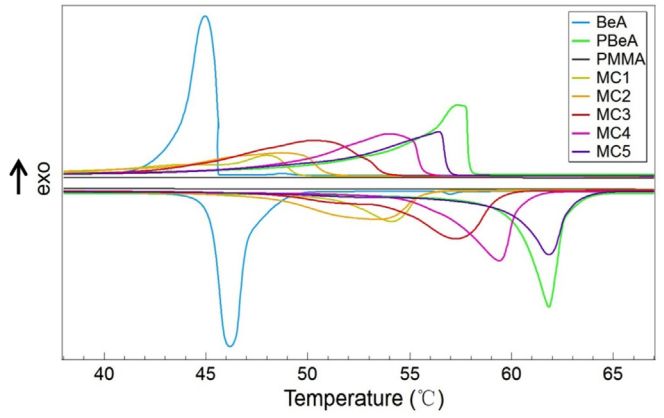

Fig. 5. DSC crystallization and melting curves of BeA, PBeA, PMMA, and P(BeA-co-MMA) microcapsules.

between microcapsules and hot stage are clearly observed. In the heating process (Fig. 6. (a)), compared to MC1, owing to the high phase change enthalpy, MC3 and MC5 effectively prolong the time to reach the setting temperature, showing that MC3 and MC5 store more thermal energy. In the temperature range of 50–60 °C, MC3 and MC5 show the peaks of slowly rising temperature, indicating that they have good thermal energy storage capacity in the temperature range. In addition, it is noted that MC3 provides a thermoregulation property near 55 °C, which is approximately 4 °C lower than MC5 owing to their differences in phase change temperatures and monomer ratios. In the cooling process (Fig. 6. (b)), the temperature dropping peaks of microcapsules after approximately 60 °C are also apparently observed, indicating that microcapsules have good thermal energy release capacity. The temperature ranges in which MC5, MC3, and MC1 show good thermal energy release capacity are 60–56 °C, 58–52 °C and 52–48 °C, respectively. These results are consistent with DSC results mentioned above.

3.4. Crystallization behaviour

The crystallization behaviour determines the energy storage capacity. The X-ray diffraction patterns of BeA, PBeA and microcapsules MC1, MC3, and MC5 are shown in Fig. 7 (a) and (b). There are three strong diffraction peaks at 2θ of 24.04° (d-spacing = 3.70 Å), 21.94° (4.05 Å) and 19.46° (4.56 Å) for monomer BeA (Fig. 7(a)). These diffraction peaks indicate that BeA can form a good crystal structure, which ensures great potential to provide energy storage capacity. In addition, PBeA and all microcapsules show a single intense diffraction peak at 2θ of 21.94° (4.05 Å) (Fig. 7 (b)), which indicates that P(BeA-co-MMA) can form good crystals at room temperature. By comparing the diffraction peaks of MC1, MC3, and MC5 at 2θ of 21.94°, it can be seen that the peak intensity increases with increasing ratio of BeA. Introduction of amorphous MMA decreases the crystallinity of the copolymer, resulting in the lowering of T_m and T_c, which is also evidenced by the DSC results.

3.5. Thermal stability

The thermal stability property is another important parameter for PCMs and should be known before pre-process applications. The thermal degradation temperature determines the processing methods of the final composite materials. The TGA curves of BeA, PBeA, PMMA and microcapsules MC1, MC3, and MC5 are shown in Fig. 8. The thermal degradation temperatures summarized from TGA results are listed in Table 2. PMMA continuously degrades in the temperature range from 180 to 430 °C, showing poor thermal stability. Compared to BeA with 5% weight loss temperature ($T_{5\%}$) of 220 °C, PBeA has a higher $T_{5\%}$ than 310 °C. Except for MC1, all other P(BeA-co-MMA) microcapsules have quite high $T_{5\%}$ and 50% weight loss temperature ($T_{50\%}$), greater than 315 °C and 390 °C, respectively, indicating that they have excellent thermal durability.

According to the above TGA results, it is obvious that the degradation temperatures of P(BeA-co-MMA) microcapsules are higher than the melting points of almost all general polymers. For example, the melting point of acrylonitrile-butadiene-styrene copolymer (ABS) is 220–240 °C, and that of polylactide acid (PLA) is 185 °C, polypropylene (PP) is 170 °C, polyethylene terephthalate (PET) is 255 °C and polyamide 66 (PA66) is 260 °C. Our P(BeA-co-MMA) microcapsules have enough thermal durability to be used as functional fillers to blend with all the above general thermal plastic polymers to develop energy storage composite materials. Furthermore, by introducing our highly thermal-durable P(BeA-co-MMA) microcapsules into ABS or PLA, which are used as the dominant materials for fused deposition molding type 3D-printing, it is greatly expected that the possibility of developing 3D printable energy storage materials can be explored.

Table 1
Thermal properties of BeA, PBeA, and P(BeA-co-MMA) microcapsules measured by DSC.

Sample	Crystallization		Melting		First heating		ΔH_{test} ($J \cdot g^{-1}$)
	T_c (°C)	ΔH_c ($J \cdot g^{-1}$)	T_m (°C)	ΔH_m ($J \cdot g^{-1}$)	T_1 (°C)	ΔH_1 ($J \cdot g^{-1}$)	
BeA	45.0	143.0	46.2	140.1	–	–	–
PBeA	57.4	115.6	61.8	114.3	62.9	116.6	115.0
MC1	48.0	56.1	54.1	56.5	56.2	68.1	56.3
MC2	48.8	74.4	53.4	75.7	56.3	93.1	75.1
MC3	50.4	105.2	57.3	104.9	57.8	115.9	105.1
MC4	54.0	102.0	59.4	100.7	60.4	114.3	101.4
MC5	56.4	98.2	61.8	97.0	62.2	108.4	97.6

T_c: crystallization temperature, ΔH_c: enthalpy of crystallization process, T_m: melting temperature, ΔH_m: enthalpy of melting process, T_1: melting point of first heating process, ΔH_1: enthalpy of first heating process, ΔH_{test}: the average phase change enthalpy of crystallization and melting processes.

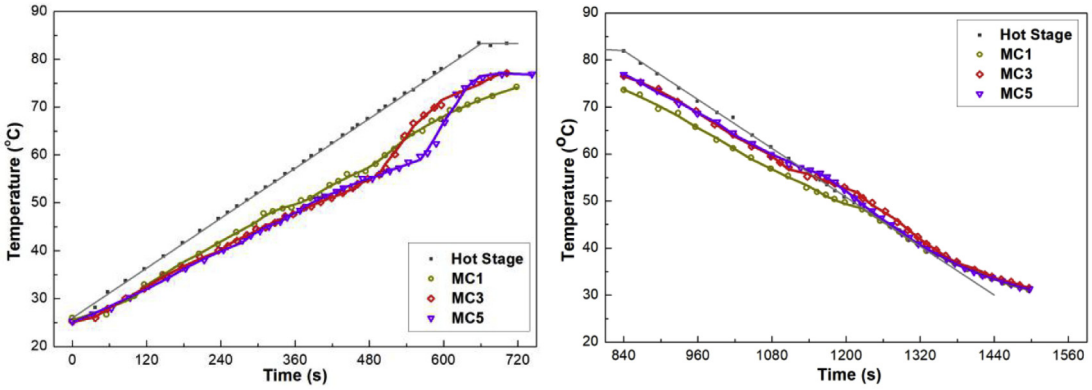

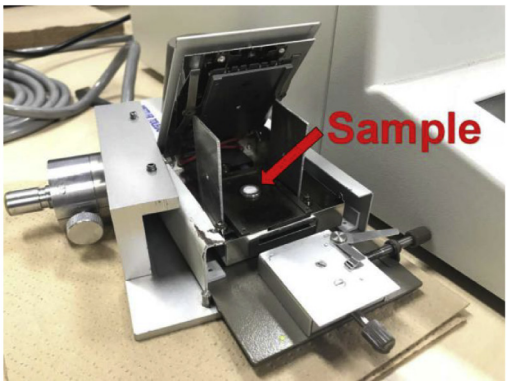

Fig. 6. Temperature change as a function of time detected by infrared thermal graphic camera for P(BeA-co-MMA) microcapsules in the heating (a) and cooling (b) cycles. The thermoregulation property of microcapsules was carried out on a hot stage (c) with a temperature change rate of 5 °C·min^{-1}.

3.6. Comparison with other PCMs in prior literature

Most PCMs reported in prior literature are encapsulated PCMs. Their low thermal reliability strongly limits their applications for extended use. There are two main reasons. One is the low stability of polymer shells. The other is shell breakage due to evaporation, sublimation, or decomposition of core materials [24]. For example, microencapsulated paraffin displays a typical two-step mass loss that can be found in its TGA curve [25]. The first mass loss resulting from thermal degradation of the paraffin occurs between 150 and 250 °C, which greatly increases the vapor pressure on the shell layer. The degradation of paraffin at low temperatures would inevitably destroy the core-shell structure and cause a loss and leakage of core materials. Not only paraffin but also almost all *n*-alkane and other aliphatic phase change compounds face the same problems.

Various methods have been used to modify the shell to improve its thermal stability. We summarized some representative methods reported in the literature for synthesis of high-thermal-stability microcapsules and listed them in Table 3 Through a heat-treating process to remove the volatile molecules, an expansion space formed inside the microcapsules could reduce the pressure core

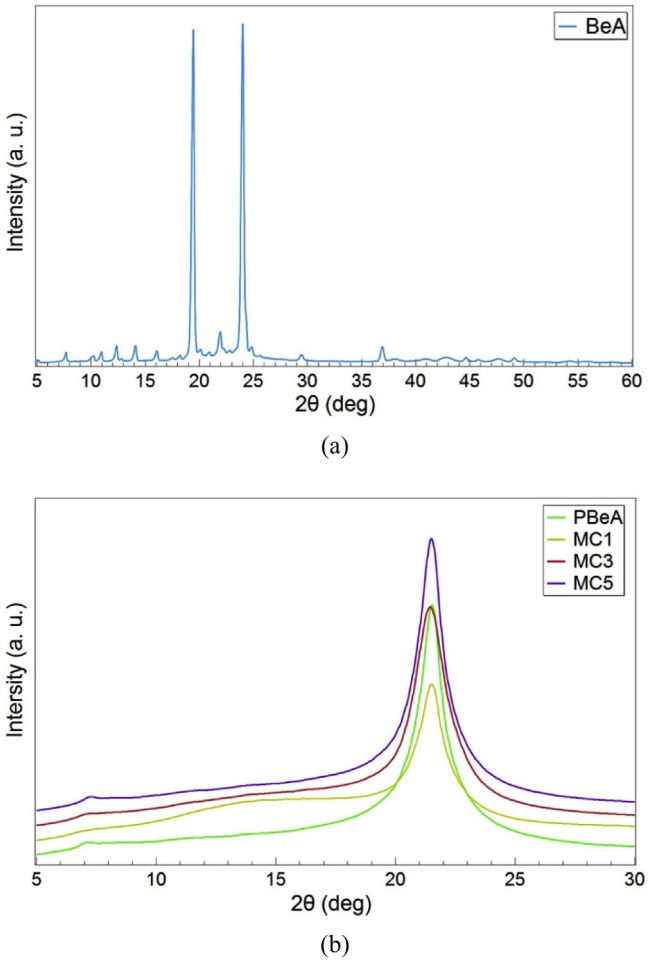

Fig. 7. WAXS patterns of BeA (a), PBeA and P(BeA-co-MMA) microcapsules (b).

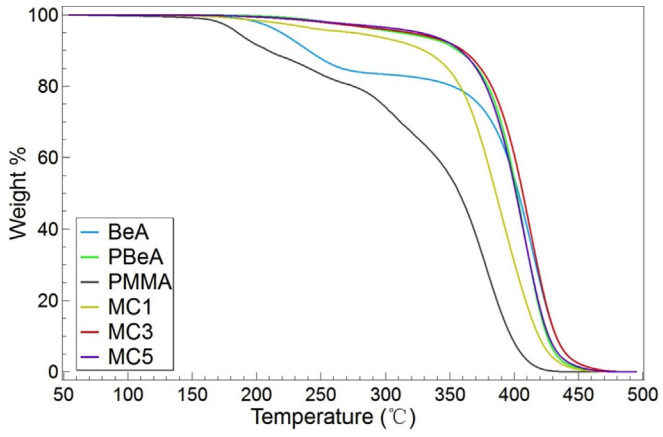

Fig. 8. TGA curves of BeA, PBeA, PMMA and P(BeA-co-MMA) microcapsules under a nitrogen atmosphere.

vapor on the shell and increase the degradation temperature to 230 °C and 289 °C in air and nitrogen, respectively. However, the average attenuation of enthalpy after heattreatment was as high as 34–54% [11]. Another method to improve the thermal stability of microcapsules is to increase the compaction factor and the physical strength of the shell layer. A crosslinked poly(lauryl methacrylate) (PLMA) shell increased the thermal degradation to 232 °C [12]. It

Table 2
Thermal stability of BeA, PBeA, PMMA, and P(BeA-co-MMA) microcapsules measured by TGA.

Sample	$T_{5\%}$ (°C)	$T_{50\%}$ (°C)
BeA	220.0	403.8
PBeA	312.3	402.0
PMMA	185.3	356.7
MC1	262.6	386.0
MC3	318.5	406.5
MC5	326.5	401.1

$T_{5\%}$: 5% weight loss temperature, $T_{50\%}$: 50% weight loss temperature.

was reported that a double-shell structure could improve the thermal stability too. $T_{5\%}$ reached 236 °C, which was 30 °C higher than that of the single shell [18]. Other researchers have reported that introducing inorganic compounds to synthesize hybrid shell microcapsules is also an effective method [17,26], but the effects are not as good. $T_{5\%}$ of aminoplast microcapsules incorporated with 3 wt% silver nano-particles is low (200 °C), and the ΔH was not given [10].

These methods reported in prior literature successfully improved the thermal durability of microcapsules to some extent but not sufficiently to withstand the general polymer processing temperature. Furthermore, most of the above methods are at the cost of attenuation of enthalpy or energy storage density. In our work, P(BeA-co-MMA) copolymer microcapsules were designed and achieved excellent thermal durability and high thermal storage capacity simultaneously (MC3, $T_{5\%} = 318.5$ °C, $\Delta H = 105.1$ J g^{-1}, in Table 3). The high energy storage capacity is provided by the phase change of long *n*-alkane side chain crystals (Fig. 1). In addition, as shown in Fig. 1, the polymer main chains act as the shell (or skeleton structure) on a nano-scale and side chains as the core that will no longer change into liquid or gas. Even if the microcapsules break into pieces, the strong interaction force between shell and core parts overcomes the shortages of shell fracture, core leakage, core evaporation, and sublimation in conventioinal microcapsules. Therefore, the excellent thermal durability of P(BeA-co-MMA) microcapsules was also realized.

4. Conclusions

Specially designed copolymer P(BeA-co-MMA) microcapsules are successfully synthesized from BeA and MMA through suspension polymerization with median diameters ranging from 7.15 to 14.46 μm. The crystalline side chains of copolymer derived from the long alkane chains of BeA provide a phase change capacity of microcapsules. The amorphous side chains of copolymer derived from pendent groups of MMA adjust the phase change temperature and increase the strength of microcapsules. Unlike conventional microcapsules, no separated surface layer is observed between the shell and core parts of the P(BeA-co-MMA) microcapsules. The problems of shell fracture, core leakage, core evaporation or sublimation, and low thermal stability in conventional microcapsules are fully resolved. According to the DSC and energy storage capacity and thermoregulation evaluation results, the high thermal durability and high energy storage capacity of P(BeA-co-MMA) microcapsules in temperature range of 48–62 °C are confirmed. Among all, MC3 shows the highest ΔH of 105.1 J g^{-1}, and its $T_{5\%}$ is more than 315 °C. MC3 has enough high thermal durability resistance to the general polymer processing temperature and is suitable to develop energy storage composite materials as functional fillers. P(BeA-co-MMA) microcapsules prove to be promising materials to store low-temperature (40–70 °C) thermal energy.

Table 3
Comparison of thermal stability and thermal storage capacity of encapsulated PCMs in prior literature.

PCMs (core)	Shell designs	$T_{5\%}$ (°C)	ΔH (J·g^{-1})	Research
Paraffin	PMMA	150	75.9	[27]
Stearic acid	Diatomite	192	57.1	[28]
Bromo-hexadecane	Aminoplast with Ag-NPs	200	N/A	[10]
CNT graft stearyl alcohol	UF	216	47.7	[9]
n-octadecane	Crosslinked PLMA	232	113.5	[12]
n-octadecane	Crosslinked Poly(MAA-co-MMA)	236	110.5	[13]
Lauryl alcohol	MF double-shell	236	155.0	[18]
n-octadecane	MF	289	57.0	[11]
P(BeA-co-MMA) copolymer microcapsule (MC3)		319	105.1	This work

ΔH: average enthalpy of crystallization and melting processes.

Acknowledgments

The authors would like to thank Professor Mitsumasa Kimata of Yamagata Univeristy for assistance with laser diffraction spectrometry measurement. This work was financially supportted by JSPS KAKENHI (Grant Number 25810123), the MEXT Program that supports the research activities of female researchers, and the Cooperative Research Program of Network Joint Research Center for Materials and Devices (2016YFA0201702), and National Key Research and Development Program of China (2016YFA0201700).

References

[1] A. Yataganbaba, B. Ozkahraman, I. Kurtbas, Worldwide trends on encapsulation of phase change materials: a bibliometric analysis (1990–2015), Appl. Energy 185 (1) (2017) 720–731.
[2] J. Pereira da Cunha, P. Eames, Thermal energy storage for low and medium temperature applications using phase change materials – a review, Appl. Energy 177 (2016) 227–238.
[3] Y. Zhang, L. Wang, B. Tang, R. Lu, S. Zhang, Form-stable phase change materials with high phase change enthalpy from the composite of paraffin and cross-linking phase change structure, Appl. Energy 184 (2016) 241–246.
[4] P. Lv, C. Liu, Z. Rao, Experiment study on the thermal properties of paraffin/kaolin thermal energy storage form-stable phase change materials, Appl. Energy 182 (2016) 475–487.
[5] A.M. Borreguero, J.L. Valverde, J.F. Rodríguez, A.H. Barber, J.J. Cubillo, M. Carmona, Synthesis and characterization of microcapsules containing Rubitherm®RT27 obtained by spray drying, Chem. Eng. J. 166 (1) (2011) 384–390.
[6] M. Malekipirbazari, S.M. Sadrameli, F. Dorkoosh, H. Sharifi, Synthetic and physical characterization of phase change materials microencapsulated by complex coacervation for thermal energy storage applications, Int. J. Energy Res. 38 (11) (2014) 1492–1500.
[7] Z. Chen, L. Cao, G. Fang, F. Shan, Synthesis and characterization of microencapsulated paraffin microcapsules as shape-stabilized thermal energy storage materials, Nanoscale Microscale Thermophys. Eng. 17 (2) (2013) 112–123.
[8] M. Silakhori, M. Naghavi, H. Metselaar, T. Mahlia, H. Fauzi, M. Mehrali, Accelerated thermal cycling test of microencapsulated paraffin wax/polyaniline made by simple preparation method for solar thermal energy storage, Materials 6 (5) (2013) 1608–1620.
[9] M. Li, M. Chen, Z. Wu, Enhancement in thermal property and mechanical property of phase change microcapsule with modified carbon nanotube, Appl. Energy 127 (2014) 166–171.
[10] Q. Song, Y. Li, J. Xing, J.Y. Hu, Y. Marcus, Thermal stability of composite phase change material microcapsules incorporated with silver nano-particles, Polymer 48 (11) (2007) 3317–3323.
[11] X.X. Zhang, X.M. Tao, K.L. Yick, Y.F. Fan, Expansion space and thermal stability of microencapsulatedn-octadecane, J. Appl. Polym. Sci. 97 (1) (2005) 390–396.
[12] X. Qiu, L. Lu, J. Wang, G. Tang, G. Song, Fabrication, thermal properties and thermal stabilities of microencapsulated n-alkane with poly(lauryl methacrylate) as shell, Thermochim. Acta 620 (2015) 10–17.
[13] X.L. Shan, J.P. Wang, X.X. Zhang, X.C. Wang, Formaldehyde-free and thermal resistant microcapsules containing n-octadecane, Thermochim. Acta 494 (1–2) (2009) 104–109.
[14] Y. Ma, J. Zong, W. Li, L. Chen, X. Tang, N. Han, J. Wang, X. Zhang, Synthesis and characterization of thermal energy storage microencapsulated n-dodecanol with acrylic polymer shell, Inside Energy 87 (2015) 86–94.
[15] X. Jiang, R. Luo, F. Peng, Y. Fang, T. Akiyama, S. Wang, Synthesis, characterization and thermal properties of paraffin microcapsules modified with nano-Al2O3, Appl. Energy 137 (2015) 731–737.
[16] A. Sarı, C. Alkan, D. Kahraman Döğüşcü, A. Biçer, Micro/nano-encapsulated n-heptadecane with polystyrene shell for latent heat thermal energy storage, Sol. Energy Mater. Sol. Cell. 126 (2014) 42–50.
[17] M. Williams, B. Olland, S.P. Armes, P. Verstraete, J. Smets, Inorganic/organic hybrid microcapsules: melamine formaldehyde-coated Laponite-based Pickering emulsions, J. Colloid Interface Sci. 460 (2015) 71–80.
[18] J.-F. Su, L.-X. Wang, L. Ren, Z. Huang, Mechanical properties and thermal stability of double-shell thermal-energy-storage microcapsules, J. Appl. Polym. Sci. 103 (2) (2007) 1295–1302.
[19] H. Zhang, X. Wang, Synthesis and properties of microencapsulated n-octadecane with polyurea shells containing different soft segments for heat energy storage and thermal regulation, Sol. Energy Mater. Sol. Cell. 93 (8) (2009) 1366–1376.
[20] S. Lu, J. Xing, Z. Zhang, G. Jia, Preparation and characterization of polyurea/polyurethane double-shell microcapsules containing butyl stearate through interfacial polymerization, J. Appl. Polym. Sci. 121 (6) (2011) 3377–3383.
[21] X. Qiu, G. Song, X. Chu, X. Li, G. Tang, Microencapsulated n-alkane with p(n-butyl methacrylate-co-methacrylic acid) shell as phase change materials for thermal energy storage, Sol. Energy 91 (2013) 212–220.
[22] L. Sánchez, E. Lacasa, M. Carmona, J.F. Rodríguez, P. Sánchez, Applying an experimental design to improve the characteristics of microcapsules containing phase change materials for fabric uses, Ind. Eng. Chem. Res. 47 (23) (2008) 9783–9790.
[23] S. Yoshio, F. Kiyoshige, Solid-state polymerization of long-chain vinyl compounds. IV. Effects of chain length on the polymorphic behavior and post-polymerization of n-alkyl methacrylates, J. Polym. Sci. Polym. Chem. Ed. 18 (1980) 2437–2494.
[24] A. Sarı, C. Alkan, C. Bilgin, Micro/nano encapsulation of some paraffin eutectic mixtures with poly(methyl methacrylate) shell: preparation, characterization and latent heat thermal energy storage properties, Appl. Energy 136 (2014) 217–227.
[25] S.I. Golestaneh, A. Mosallanejad, G. Karimi, M. Khorram, M. Khashi, Fabrication and characterization of phase change material composite fibers with wide phase-transition temperature range by co-electrospinning method, Appl. Energy 182 (2016) 409–417.
[26] Y. Zhang, X. Wang, D. Wu, Design and fabrication of dual-functional microcapsules containing phase change material core and zirconium oxide shell with fluorescent characteristics, Sol. Energy Mater. Sol. Cell. 133 (2015) 56–68.
[27] S. Ma, G. Song, W. Li, P. Fan, G. Tang, UV irradiation-initiated MMA polymerization to prepare microcapsules containing phase change paraffin, Sol. Energy Mater. Sol. Cell. 94 (10) (2010) 1643–1647.
[28] X. Fu, Z. Liu, B. Wu, J. Wang, J. Lei, Preparation and thermal properties of stearic acid/diatomite composites as form-stable phase change materials for thermal energy storage via direct impregnation method, J. Therm. Anal. Calorim. 123 (2) (2015) 1173–1181.